Mixing in the Main Thermocline

J. N. MOUM

College of Oceanography, Oregon State University, Corvallis, OR 97331

T. R. OSBORN

Chesapeake Bay Institute, Shady Side, MD 20764

(Manuscript received 11 March 1985, in final form 13 January 1986)

ABSTRACT

A series of profiles of velocity microstructure along 152°E in the western North Pacific Ocean were collected in May–June 1982. Large, averaged turbulent dissipation rates, ϵ, found in the main thermocline (400 to 1000 m) were determined by a combination of large independent estimates of ϵ and a greater rate of occurrence of turbulent events in the main thermocline than elsewhere. Concurrently we find that averaged values of ϵ exhibit a positive dependence on the buoyancy frequency, N, and that the form $\epsilon = aN^{\gamma}$ is best fit by $\gamma = 1$ when only the data below 400 m are considered. Of the more than 5000 m of data collected below 1000 m depth, 12% showed measurable turbulence and dominated the depth averages. A deep ocean estimate of an upper bound to the eddy coefficient for vertical diffusion, K_ρ, is 10^{-4} m^2 s^{-1} and not significantly different from the value estimated by Munk. The inferred dependence of the mass flux with depth indicates the relative significance of vertical mixing in the main thermocline. Other processes must influence the maintenance of the more weakly stratified 15°–18°C water above.

1. Introduction

The emphasis in the ocean microstructure field has been to study the more active regions of the ocean, generally near to the surface. Near-surface studies offer the combined blessings of greater signal levels and relative ease of rapid sampling (Caldwell et al., 1985). Deep ocean studies using vertical profilers involve added technical difficulties; high pressure enters into the design considerations of the instrumentation vehicle, a generally greater sensitivity to signal (or smaller noise level) is required than is necessary for near-surface measurements and a reliable system must be employed to transfer data over several kilometers or to store substantial amounts of data internally. In part because of these reasons, there have been few deep-ocean microstructure measurements.

Gregg (1977) reports temperature microstructure measurements from 28°N and 28°S at 155°W in the Pacific Ocean (to a maximum depth of 3600 m). The most active records were found in the seasonal thermocline and below, but not in, the main thermocline. The deepest records were not markedly different from the records in the main thermocline. Two other studies of interest are those of Lueck et al. (1983) and Gargett and Osborn (1981). In both cases, a positive scaling of turbulent kinetic energy, ϵ, on buoyancy frequency, N, was found. However, since N was a monotonic function of depth below the mixed layer in both cases, the proposed positive scaling was not convincingly different from a scaled depth dependence.

In this paper, we describe a set of velocity microstructure measurements taken in the western Pacific Ocean in early summer, 1982. Our operations were in conjunction with the recovery of a line of current meter moorings along 152°E and an associated CTD survey made during the Wespac experiment. The microstructure data encompassed a strong main thermocline and a nonmonotonic depth profile of N. In the following sections we briefly describe the instrumentation, discuss the microstructure results within the context of the accompanying measurements and attempt to convince the reader that the main thermocline is a relatively active site for turbulence. Some implications are proposed for the possible mechanisms by which the energy in the internal wave field is maintained and a deep ocean estimate (to 2200 m) for an upper bound to the vertical eddy diffusivity is made.

2. Instrumentation and data handling

Velocity microstructure measurements were made using the freely falling, internally recording instrument, Camel III. The features which distinguish this instrument from the other Camels are the internal recording system and the strengthened pressure case. Internal recording removed the need for an expendable wire link to telemeter the data to the surface and allowed drops

to 2300 m depth. The mechanical construction, the electronics and the signal processing are not substantially different from Camel II, which has been described in some detail by Lueck et al. (1983) and Moum and Lueck (1985).

The velocity microstructure data were filtered at 100 Hz, recorded onboard Camel III, digitized at 400 Hz, and rerecorded on magnetic tape after retrieval of the instrument. Spiky data were detected by a first-differencing routine and automatically removed. Blocks of 1024 data points were first-differenced and cosine-tapered. From these, spectral variance estimates were made, and the measured calibrations applied to estimate ϵ, the rate of turbulent kinetic energy dissipation. Since these estimates were computed over fixed block sizes, the vertical depth bin is related to the fall speed. At our descent speeds of 60–80 cm s^{-1}, the estimates of ϵ represent depth bins of 1.5–2 m. In all, more than 13 000 m of data were recovered (or roughly 7000 independent estimates of ϵ). Of these, more than 5000 m of data represent depths greater than 1000 m.

The key measurement for this study was of microscale shears (50 cm to 1 cm) using airfoil probes (Osborn and Crawford, 1980). From this measurement and invoking the assumption of isotropic turbulence, estimates were made of ϵ. The errors involved in the estimate of ϵ and the spectral techniques used to compute ϵ are discussed in detail by Moum (1984). The uncertainty in our estimate of ϵ arises from seven sources:

1) The uncertainty in the calibration of the electronics used to process the signal is less than 1% or, as a squared term in the expression for ϵ, no worse than 2% in ϵ.

2) The estimate of the fall rate of the instrument from electronic differentiation of the pressure signal is known to within 1.5 cm s^{-1} resulting in a worst case

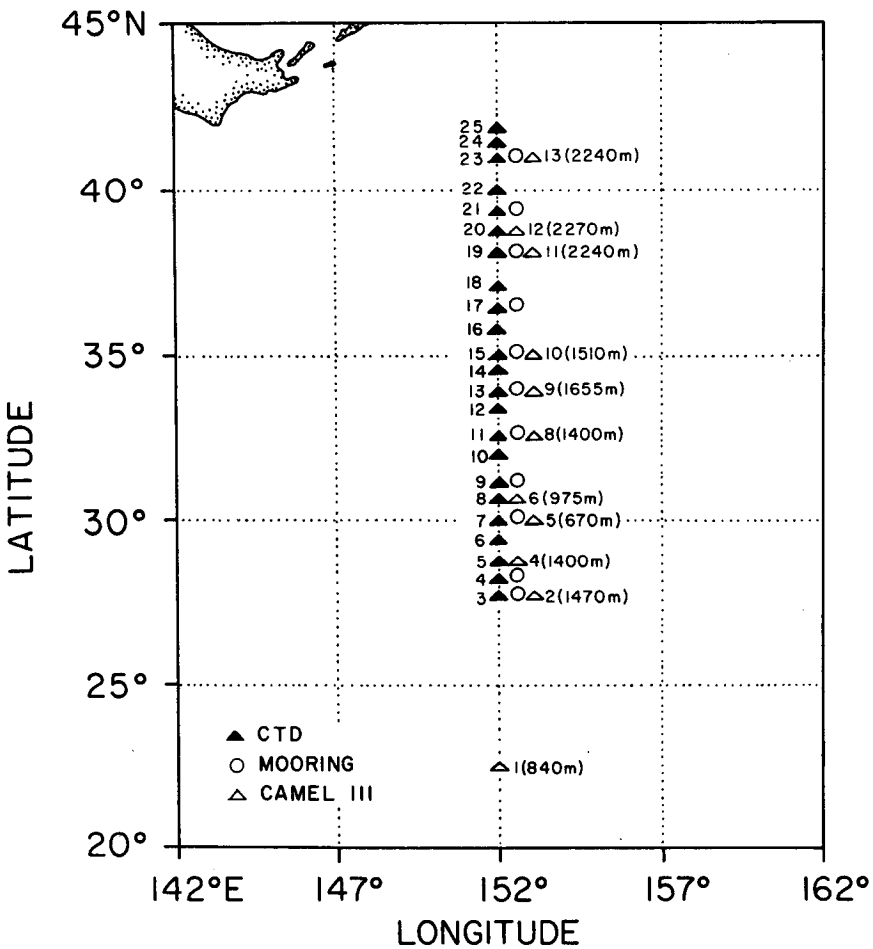

FIG. 1. Locations of Camel profiles and CTD casts made during the recovery of the Wespac line of current meter moorings in May–June 1982, along 152°E in the western North Pacific. In parentheses is noted the depth in meters of Camel profiles.

error of 2.5% at our smallest fall speeds of 60 cm s^{-1}. As a fourth power term in ϵ, this results in a 10% error in ϵ.

3) Calibration of the airfoil probes is estimated to be accurate to within 10% (S. Milaire, personal communication, 1984), leading to a 20% error in ϵ.

4) The error due to inadequate compensation for the frequency response of the electronics is 5%, or 10% in ϵ.

5) The spatial response of the probe has recently been measured by Ninnis (1984) using a laser Doppler anemometer reference. The 3 dB point for the probes used in this study was at 70 cyc m^{-1}, resulting in a 20% loss of variance at $\epsilon = 10^{-6}$ m^2 s^{-3} and less at smaller ϵ values.

6) The assumption of isotropic turbulence in a stratified flow has been examined by Gargett et al. (1984) and found to be a relatively good one under the mixing regimes discussed here. The assumption breaks down at the lower dissipation rates which do not greatly affect the depth averages. Our two independent estimates of ϵ (using two orthogonally mounted airfoil probes) indicate differences of up to a factor of three over 1.5 to 2 meter averages, while 20% to 40% differences are more usual. It is difficult to put a bound on this error, but we believe that generally, and especially for $\epsilon > 10^{-8}$ m^2 s^{-3}, it is no worse than 50%.

7) There is a nearly constant noise level of 3×10^{-10} m^2 s^{-3} in ϵ due to hydrodynamically induced vibrations of the instrument body (Moum and Lueck, 1985).

Adding the worst case errors from these recognized sources leads us to believe that we can determine ϵ to within a factor of two.

3. Section along 152°E—28° to 42°N

a. CTD

The temperature and conductivity data were collected by the WHOI CTD group. Temperature and salinity data at 2 db intervals were kindly provided by P. Niiler and are further described in Niiler et al. (1985). We calculated buoyancy frequency from these data using the International Equation of State of Seawater, 1980 (Gill, 1982).

The locations of the microstructure profiles and CTD casts along 152°E are shown in Fig. 1. The line of current meter moorings was deployed by W. Schmitz and results from the array are discussed by Schmitz et al. (1982) and Schmitz (1984).

A temperature section along 152°E derived from the CTD measurements in May and June 1982, (Fig. 2a) shows four distinct features: (i) the isotherms sloping steeply downward from the north at the north end of the section indicating the front of the Oyashio Current; (ii) the Kuroshio Extension System (the front is defined by Schmitz et al., 1982, as the location where the 15°C isotherm is at 200 m depth) positioned at 37.5°N; (iii) a cold core ringlike feature centered just north of 34°N. Although not uniquely defined as such

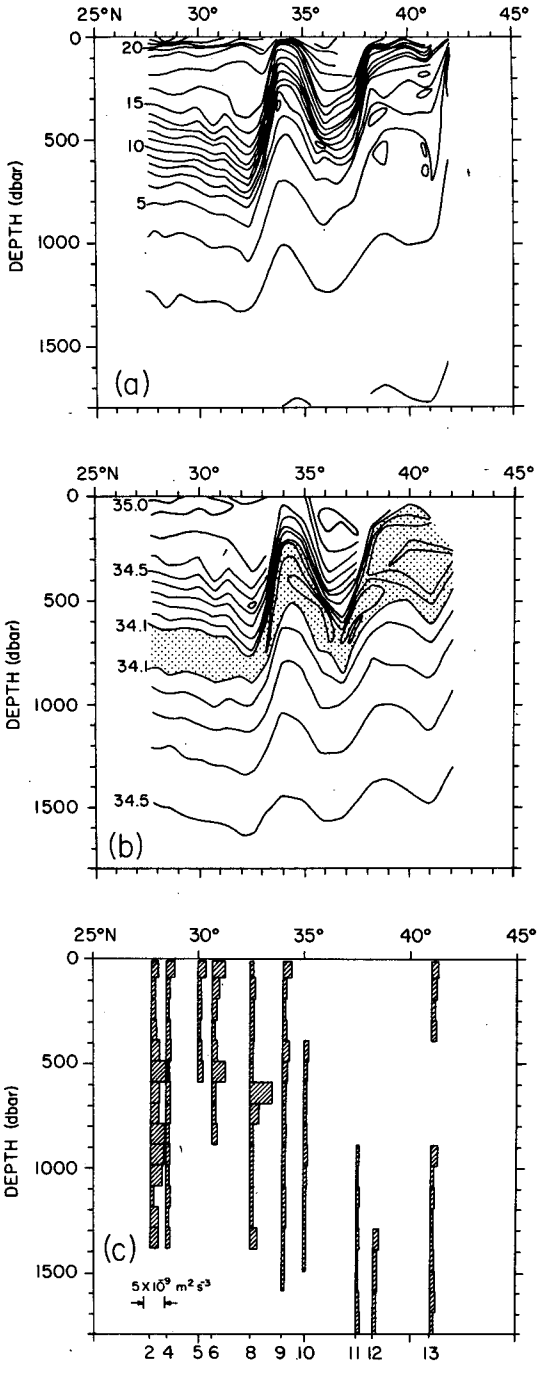

FIG. 2. (a) Temperature section along 152°E in May–June 1982; (b) salinity section along 152°E. The salinity minimum bounded by the 34.1 ppt contours is shaded. (c) 100-m averages of turbulent kinetic energy dissipation plotted on a linear scale. A reference scale of 5×10^{-9} m^2 s^{-3} is shown in the lower left. Camel profile numbers are shown at bottom.

by a single section, this feature will henceforth be referred to as a ring; (iv) a strong main thermocline south of the ring ranging from 6°C at 800 m depth to 15°C at 475 m depth at 32.5°N and sloping upwards towards the south. Associated with the lower part of the main thermocline was a salinity minimum (shaded in Fig. 2b) which apparently originates in the area of the Oyashio front. Above the main thermocline was a weakly stratified body of water (15° to 18°C).

b. *Dissipation profiles*

Microstructure profiles 2, 4, 5, 6 and 8 were made south of the ring and through the main thermocline. Profile 9 was made through the center of the cold core ring. Instrument problems limited the successful recovery of data from subsequent profiles and 10, 11, 12 and 13 are incomplete. All of these were made north of the ring. Profile 11 through the Kuroshio front only returned data from below 900 m. The results, in terms of 100 m vertical averages of ϵ, are shown in Fig. 2c. For the convenience of the reader, Fig. 2c is plotted to scale latitudinally with Figs. 2a and 2b and will be described in more detail in ensuing paragraphs. Table 1 lists shallow (20 to 400 m), thermocline (400 to 1000 m) and deep (>1000 m) averages of ϵ as well as the fraction of turbulent events with ϵ greater than three times the noise level which were encountered over those depth intervals.

For each Camel profile, a coincident profile of buoyancy frequency, N, was calculated with 25 m depth resolution. Profiles of buoyancy frequency at 27.7° and 32.5°N (both south of the ring; Figs. 3b and 4b) indicate a subsurface maximum in N of 0.006 to 0.007 rad s^{-1} associated with the main thermocline. The subsurface maximum was deeper at 32.5°N as can be inferred from the temperature section. All of the stations south of the ring showed this distinct structure in buoyancy frequency.

Drop 8 (Fig. 3a) was typical of the microstructure profiles made south of the cold core ring. In these profiles, the averages were dominated by 10–30 meter thick turbulent patches within the main thermocline. South of 34°N (south of drop 9 inside of the ring) each of the profiles of 100 m-averaged dissipation showed subsurface maxima within the main thermocline (Fig. 2c). The maxima were less obvious in drops 4 and 5 but the averaged values of ϵ within the main thermocline were still significantly larger than the vertically adjacent averaged values of ϵ just above, *but not in,* the main thermocline.

Drop 2 (Fig. 4a) is interesting due to the relatively low values of averaged dissipation encountered in the upper part of the water column ($\bar{\epsilon} = 7 \times 10^{-10}$ m^2 s^{-3} over the upper 400 m) in contrast to the larger averaged value of 21×10^{-10} m^2 s^{-3} over the depth range 400–1000 m (see Table 1). The 400–1000 m value was considerably larger than the dataset-averaged value of 9×10^{-10} m^2 s^{-3} due to a relatively larger fraction of turbulent events in the water column. For drop 2, 41% of independent estimates of ϵ were larger than 10^{-9} m^2 s^{-3} over the 400–1000 m depth range as compared to 22% for the entire dataset over this depth range.

The presence of the salinity minimum at the bottom of the main thermocline suggests a suitable site for salt fingering. Unfortunately, we cannot determine the importance of this phenomenon from our measurements. In our records there is no suggestion of the amplitude- and band-limited temperature gradient signal which is associated with salt fingers (Gargett and Schmitt, 1982) and which we have seen in our recent equatorial measurements (Moum et al., 1986). Generally, it is difficult

TABLE 1. Values of the rate of dissipation of turbulent kinetic energy averaged over the three indicated depth ranges.*

Camel profile	Latitude	(20–400 m) ϵ ($\times 10^{-10}$) m^2 s^{-3}	(20–400 m) $>10^{-9}$ m^2 s^{-3}	(400–1000 m) ϵ ($\times 10^{-10}$) m^2 s^{-3}	(400–1000 m) $>10^{-9}$ m^2 s^{-3}	(>1000 m) ϵ ($\times 10^{-10}$) m^2 s^{-3}	(>1000 m) $>10^{-9}$ m^2 s^{-3}
1	22.7°N	32.	0.59	7.	0.23	—	—
2	27.7	7.	0.19	21.	0.41	14.	0.42
4	28.5	8.	0.23	5.	0.15	6.	0.19
5	30.	6.	0.22	5.	0.18	—	—
6	30.7	14.	0.23	12.	0.30	—	—
8	32.5	3.	0.08	12.	0.24	6.	0.16
9	34.	8.	0.26	6.	0.15	4.	0.11
10	35.	—	—	3.	0.09	2.	0.03
11	37.5	—	—	5.	0.21	4.	0.09
12	38.3	—	—	—	—	3.	0.06
13	41.	12.	0.47	—	—	3.	0.07

* Individual estimates of ϵ which were less than the noise level were set = 0 so that these averages represent lower bounds. The fraction of the dissipation values greater than 10^{-9} m^2 s^{-3} (or three times the noise level) is an indication of the fraction of the water column which is actively and measurably turbulent.

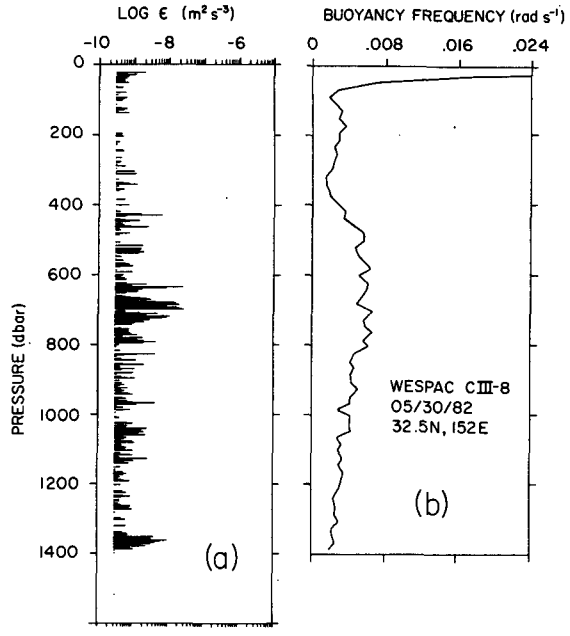

FIG. 3. (a) Profile of turbulent kinetic energy dissipation, ϵ, at 32.5°N plotted as base 10 logarithm vs depth. Each bar represents a 1.5–2 m depth average of ϵ. Missing data are due to noise contamination in both shear channels. (b) Profile of buoyancy frequency, N, from a nearly coincident CTD cast.

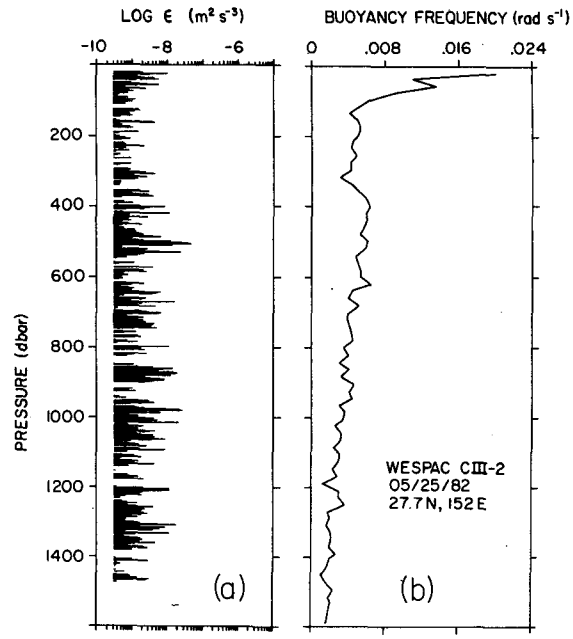

FIG. 4. As in Fig. 3 but at 27.7°N.

to detect fingering with a vertical profiler since the signature of the salt fingers is essentially horizontal (Schmitt and Evans, 1979). Larson and Gregg (1983) pointed out a number of instances where the finestructure field was suitable for salt fingering and the dissipation of turbulent kinetic energy was much greater than the estimated buoyancy flux, suggesting that the production of turbulent energy was due to other sources.

Drop 9 made within the cold core ring was relatively inactive. The deep portions (to 2300 m) of drops 11, 12 and 13 were similarly inactive. It is noteworthy, however, that measurable turbulence does occur below 2000 m. In fact, we recorded a single 30 m thick turbulent patch centered at 2030 m depth in drop 11 with a patch-averaged dissipation of 3×10^{-9} m^2 s^{-3} (or ten times the instrument's noise level).

4. Discussion

a. Turbulent kinetic energy ϵ and eddy kinetic energy

The Wespac study region was energetically dominated by the Kuroshio Extension Current and the cold core ring. A reasonable question, then, is to ask how this relates to the energy dissipated at the scales of three-dimensional turbulence. Schmitz (personal communication, 1985) has computed eddy kinetic energy, K_E, using the mean values of the horizontal velocity components measured by moored current meters that were deployed in early summer, 1981, and recovered in early summer, 1982. The data were low-pass filtered at two days and averaged over 12 months. We present Fig. 5a as a representation of the horizontal and vertical structure of the kinetic energy in the field of mesoscale-type motions estimated from the 1981/82 moorings at two depth intervals (600 and 1200 m). Figure 5b represents dissipation values averaged over three depth intervals (we have included a 250–300 m average to compare to Schmitz et al., 1982). The comparison is meant to

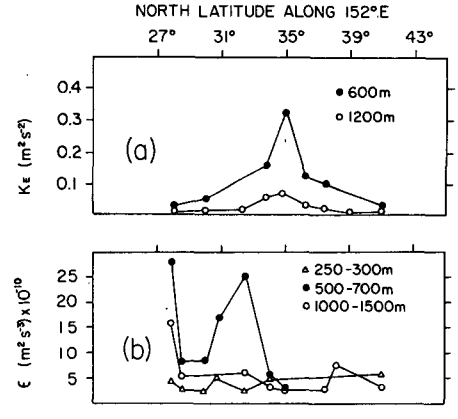

FIG. 5. (a) Averages of eddy kinetic energy over the period early summer 1981 to early summer 1982, from current meters at 600 and 1200 m depth along 152°E. (Courtesy of W. Schmitz.) (b) Averages of ϵ over the depth ranges 250–300 m, 500–700 m and 1000–1500 m for single Camel profiles made in May/June 1982.

be qualitative, since neither are the respective measurements coincident, nor have they been comparably averaged. While the K_E estimates are year-long averages, the dissipation profiles represent spatial snapshots through an intermittently turbulent field.

Two distinct trends are obvious in the latitudinal section of K_E. First of all, K_E increased northward from 28°N to peak values at or just north of the position of the cold-core ring (which was centered at 34.5°N in May, 1982). In each case, the peak value was about a factor of ten greater than the value at 28°N. Second, at each mooring site, vertically adjacent and deeper meters recorded values of K_E which were smaller by up to a factor of ten. This was also true for the 1980/81 data presented by Schmitz et al. (1982) and which includes K_E estimates from shallower current meters at 250–300 m.

These two trends were not apparent in the ϵ-section. In fact, the 500–700 m (mid-depth) values of ϵ were the largest for every single drop south of the ring and these peaked about 2° south of the ring (or 2° south of the peak in K_E). No apparent latitudinal peak occurred in either of the 250 to 300 m or the 1000–1500 m segments. Drop 9, which was made directly through the ring, actually exhibited some of the smallest values of $\bar{\epsilon}$. These results imply that there is no reason to suggest a relation between the turbulence levels and the averaged kinetic energy in the eddy field.

b. *Turbulent kinetic energy ϵ and buoyancy frequency N*

The suggestion from Figs. 2, 3, 4 and 5 is that the turbulence in the main thermocline is both more intense and more frequently occurring than elsewhere. In this section, we examine this behavior more closely through a comparison between the measured turbulence parameter, ϵ, and the buoyancy frequency, N.

Averages of N (with 25 m depth resolution) over the five microstructure profiles made south of the cold core ring (2, 4, 5, 6, 8) are shown in Fig. 6. The main thermocline is distinguished by a peak in $\bar{N}$ at 500 m depth that is more than twice the value of the local minimum at 300 m. The value at 300 m is approximately equal to that at 900 m, below which $\bar{N}$ gradually decreases.

To compare to the vertical profile of $\bar{N}$, individual estimates of ϵ were averaged over 25 m depth intervals and then averaged over the five drops south of the ring (Fig. 7). Each point plotted represents 35 to 45 independent estimates of ϵ. The minimum in turbulent activity between 200 and 400 m stands out distinctly since the seven adjacent points in the range 200–400 m are the smallest values over the entire depth range to 1350 m (averaging was not done below 1350 m since only drop 2 was deeper while at least three drops were averaged into the remainder of the points). The maximum value of $\bar{\epsilon}$ was at 500 m and was larger than the shallowest value. Below 500 m, there was considerable variability in $\bar{\epsilon}$, adjacent 25 m depth averages differing by up to a factor of six.

Qualitative agreement exists in the shapes of the two profiles in Figs. 6 and 7. The minima at 200–400 m and the maxima at 500–700 m coincide, and there is also a slow decrease with depth to 1350 m in both profiles. In short, where $\bar{N}$ was large in the water column, $\bar{\epsilon}$ was also large and $\bar{\epsilon}$ was small where $\bar{N}$ was small. However, $\bar{\epsilon}$ was considerably more variable in space (and presumably time) than $\bar{N}$. As well, for the same value of $\bar{N}$ above and below the main thermo-

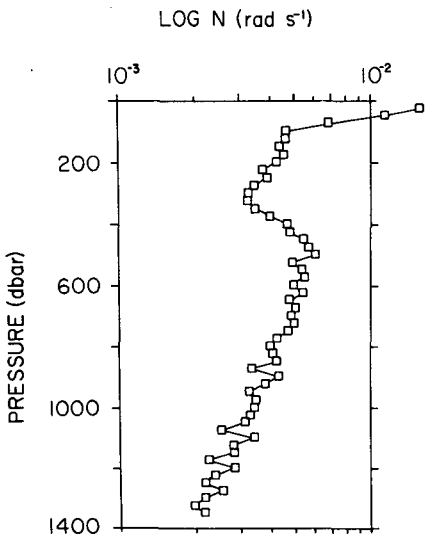

FIG. 6. Averaged profile of N from 5 CTD casts at 27.7°, 28.5°, 30°, 30.7° and 32.5°N along 152°E in May 1982.

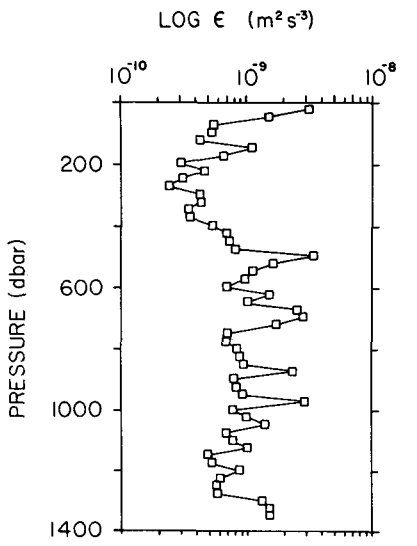

FIG. 7. Averages over 25 m of ϵ from 5 Camel profiles at the locations of, and coincident with, the CTD casts in Fig. 6.

cline, Fig. 7 shows estimates of $\bar{\epsilon}$ which differed by a factor of almost ten.

Averaged values of ϵ were larger in the main thermocline not only because individual estimates were larger (and tended to dominate the average) but also because turbulent patches occurred more frequently. The fraction of individual estimates of ϵ which was greater than a fixed value were counted in 50 m depth bins for the five drops south of 34.5°N (Fig. 8). From 500–800 m depth, 30 to 40% of the values were greater than 10^{-9} m^2 s^{-3} while 5 to 20% were greater than 3×10^{-9} m^2 s^{-3}. In this depth range (encompassing the main thermocline), the number of turbulent patches found was 4 to 5 times greater than in the 200–400 m depth range.

Coincident 25 meter depth estimates of N and ϵ (all data included here; open circles in Fig. 9) were averaged over ⅓ decade intervals in N and plotted as mean ± 2 standard errors ($\pm 2\sigma/\sqrt{n}$; 95% confidence interval of the mean). Actual errors in the computation of N are confined to the symbols while errors in computing ϵ fall within the spread of the data as expressed in Fig. 9. The best fit of the points to the form $\epsilon = aN^\gamma$ yields $a = 3.8 \times 10^{-8}$, $\gamma = 0.70$. Maximum and minimum slopes falling within all of the data spread bars give $a = 1.2 \times 10^{-7}$, $\gamma = 0.91$ and $a = 8.0 \times 10^{-9}$, $\gamma = 0.44$. The 25 meter ϵ, N pairs were reaveraged over ⅓ decade intervals in N to include only those data from depths greater than 400 m (i.e., only main thermocline and deeper values; open triangles in Fig. 9). The best fit to these points yields $a = 2.3 \times 10^{-7}$ and $\gamma = 1.0$. Maximum and minimum slopes falling within 2 standard errors of the mean give $a = 7.5 \times 10^{-7}$, $\gamma = 1.2$ and $a = 3.4 \times 10^{-8}$, $\gamma = 0.7$. In either case, the slope is distinctly positive. When only those data taken from or below the main thermocline are considered, the slope is indistinguishable from 1.

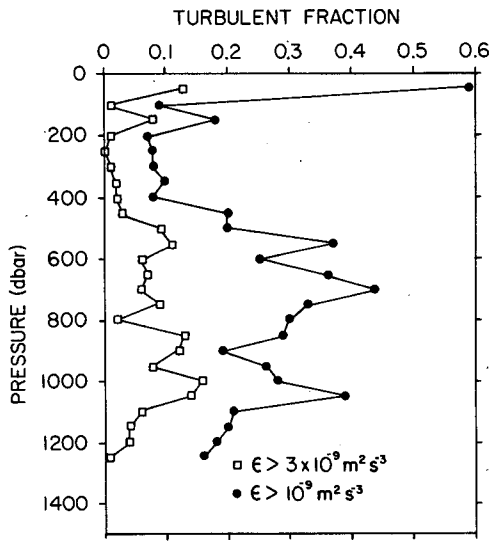

FIG. 8. Fraction of data in 50 m depth bins from the five Camel profiles discussed in Fig. 7 which were greater than two threshold levels of ϵ.

Gargett and Holloway (1984) have presented a case for a positive dependence of ϵ on N based on the hypothesis that the turbulent energy is drawn from the internal wave field. They suggest a relation $\epsilon \propto N^\gamma$, where γ has a value of 1 or 1.5, depending on the appropriate scaling for the vertical velocity variance in the internal wave field. Comparison to the Gargett and Holloway hypothesis is best made by comparing only those data from or below the main thermocline. Above 400 m, the effects of surface processes cannot generally be neglected. In and below the main thermocline, however, the mixing (and hence, ϵ) may be more safely dissociated from surface effects and we might conjecture that the role played by internal waves may well be a dominant one. These data indicate a value of γ which is indistinguishable from 1 and distinctly different from 1.5.

Based on the above form for $\epsilon = aN^\gamma$ and the form of Munk (1981) to estimate the energy in the internal wave field, $E = 0.003N/N_0$ [m^2 s^{-2}] (N_0 is a surface-extrapolated value), we can make an estimate for the time scale over which the energy in the internal wave field is dissipated by turbulence, given that there is no external source to the field. This is $\tau = E/\bar{\epsilon}$ which, together with the two expressions above, yields

$$\tau = 0.003\bar{\epsilon}^{[(1/\gamma)-1]}/N_0 a^{(1/\gamma)}.$$

The best fit to the points taken from and below the main thermocline in Fig. 9 ($\gamma = 1$, $a = 2.3 \times 10^{-7}$) together with $N_0 = 0.0055$ rad s^{-1} and ϵ averaged over the main thermocline (400–1000 m) which is 8.4×10^{-10} m^2 s^{-3}, yields $\tau = 27$ days. The maximum/minimum slope estimates from Fig. 9 yield $\tau = 26/38$ days.

McComas and Müller (1981) have estimated that a time of order (50–100 days) is necessary to drain the energy of the dominant low-mode waves via wave–wave interactions. As Garrett (1984) suggests, the agreement of this time scale with the dissipation decay scale may indicate an even transfer of energy through the spectrum, thereby smoothing temporal variations in internal wave generation. In fact, our estimated decay scale is somewhat less than 50–100 days, perhaps indicating a more rapid response at the high wavenumber end of the spectrum.

The question of spatial smoothing of internal wave spectral energy levels may also be linked to this decay time scale. Garrett (1984) estimates (with an emphasis on the uncertainty of this estimate) that a patch of high wavenumber energy would spread 1000 km in 100 days and implies that this is a large enough horizontal scale to permit uniformity in the IW energy levels. We present our estimate τ as somewhat less than 100 days (as are comparable estimates made by Lueck et al., 1983,

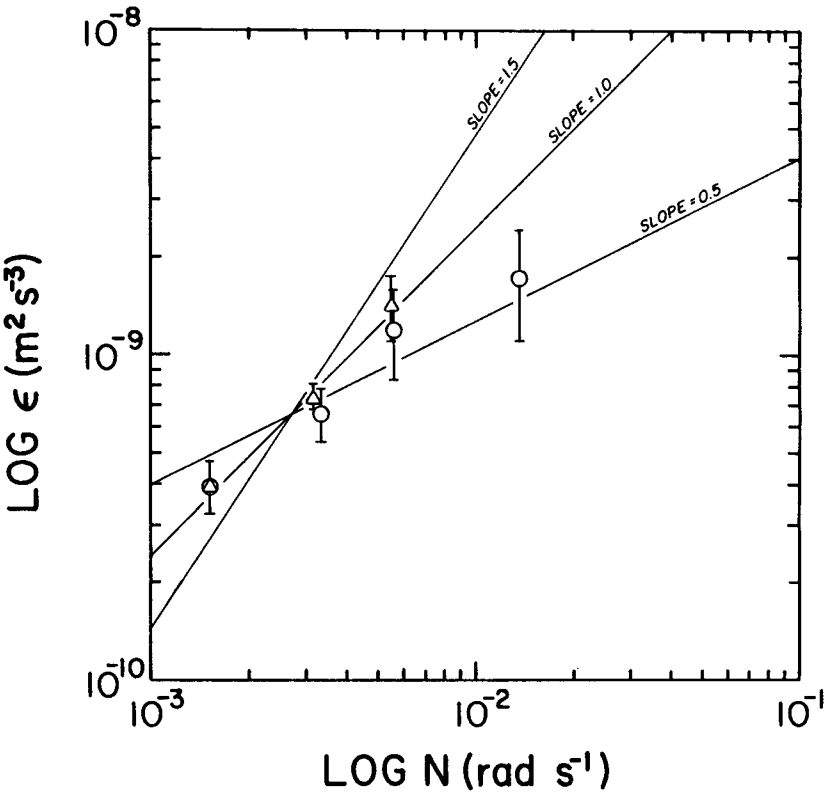

FIG. 9. Averages of ϵ over ⅓ decade intervals in N from; (i) all of the 25 m averages of ϵ and N from the Wespac data (open circles); (ii) only those data from depths greater than 400 m (open triangles). The bars represent ±2 standard errors (95% confidence interval of the mean). Lines with slopes of 0.5, 1.0 and 1.5 are drawn for comparison.

and Moum et al., 1985) and await a more reliable estimate of the horizontal spreading rate of the energy in the internal wave field.

c. *Deep-ocean estimate of K_ρ*

Using a production–dissipation–buoyancy flux balance of the turbulent kinetic energy equation, Osborn (1980) proposed an upper bound for the coefficient of vertical diffusion of density, $K_\rho < 0.2\epsilon/N^2$. Oakey (1982) tested the value of the constant coefficient and found agreement (in a mixed layer) to within a factor of two. Averages over 100 m of ϵ and N for all of the Wespac drops were used to estimate K_ρ which is plotted in Fig. 10 to 2200 m depth. An envelope of ±2 standard errors (95% confidence interval of the mean) is included to show the spread of the data.

At 900 m, K_ρ is less than 10^{-5} m^2 s^{-1}. Below 900 m, K_ρ steadily increases and is less than 5×10^{-5} m^2 s^{-1} below 2000 m. The deep estimates of K_ρ approach that of Munk (1966) who estimated a constant value of K_ρ to be about 10^{-4} m^2 s^{-1} in the deep ocean from a balance of the density equation between the upward advection of dense water and the turbulent diffusion downwards of lighter water. The balance can be expressed as

$$w\rho_z - (K_\rho \rho_z)_z = 0,$$

where the subscript z represents differentiation with respect to the vertical coordinate z. This may be rewritten (and Gargett, 1984, does this) as

$$\rho_z[w - (K_\rho)_z] - K_\rho \rho_{zz} = 0.$$

Munk (1966) assumed K_ρ to be a constant value in the deep ocean between 1 and 4 kilometers in order to simplify the analysis. With the estimates shown in Fig. 10 this assumption may be checked. By estimating the rate of formation of Antarctic Bottom Water and assuming uniform spreading and rising rates over the remainder of the world's oceans, Munk estimated a globally averaged upwelling speed, w, of 10^{-7} m s^{-1}. From Fig. 10, $(K_\rho)_z$ is estimated from the values at 500–2000 m to be 3×10^{-5} m^2 s^{-1} in 1500 m or 2×10^{-8} m s^{-1}. This is 20% of Munk's value for w and does not affect the order of magnitude estimate made for K_ρ. We note that a constant $(K_\rho)_z = 2 \times 10^{-8}$ m s^{-1} gives a value for the upper bound to K_ρ of 10^{-4} m^2 s^{-1} at a few thousand meters.

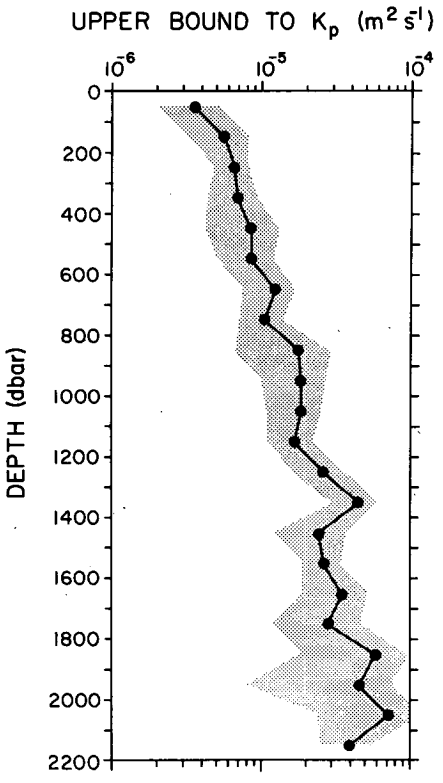

FIG. 10. Upper bound to the vertical eddy viscosity, K_ρ, as defined by Osborn (1980). The stippled envelope represents ±2 standard errors of the mean value of K_ρ computed from individual 25 m estimates of ϵ and N and then averaged over 100 meter bins for all of the Wespac data.

We have estimated a form for K_ρ which increases with depth below the main thermocline and find it instructive to argue that the buoyancy flux decreases with depth below the main thermocline.

The ratio of the buoyancy flux to ϵ may well be fixed by a constant flux Richardson number (Osborn, 1980; Oakey, 1982) whereby approximately 80% of the locally-produced turbulent kinetic energy is dissipated while the remaining 20% goes to raising the potential energy via a buoyancy flux. A positive dependence, $\epsilon \propto N^\gamma$ ($\gamma > 0$), implies a similar form for the buoyancy flux, which then decreases with depth as N decreases.

The preceding argument requires a maximum buoyancy flux in the main thermocline and a local minimum in the buoyancy flux in the 15°–18°C water above the main thermocline (Figs. 2a, 6, 7). From this, we must emphasize the importance of vertical mixing across the main thermocline as opposed to other processes in the 15°–18°C water immediately above. Talley and Raymer (1982) point out the importance of deep wintertime convection in maintaining the 18° water in the western North Atlantic, a process which may also be important in the western North Pacific.

5. Summary

These measurements of the rate of dissipation of turbulent kinetic energy are unique in providing a sample of turbulence in a deep main thermocline. In an averaged sense, $\bar{\epsilon}$ has a positive dependence on $\bar{N}$. Ensemble averages over bins of N from or below the main thermocline indicate that a form $\epsilon = aN^\gamma$ is best represented by $\gamma = 1$. Averages of ϵ are dominated by thick patches (and/or frequently-occurring thin patches) of relatively low-level (not more than two factors of ten greater than the noise level) turbulence. This implies that, if the turbulence is a direct result of energy transferred from the internal wave field, the positive dependence of ϵ and N results from a greater breaking rate of internal waves where N is large (i.e., in the main thermocline). Furthermore, a comparison of Figs. 6 and 7 implies that, while ϵ and N display a similar shape with depth, the dissipation rate is not a single-valued function of N.

The positive ϵ–N dependence implies (based on turbulent energy balance arguments) that the turbulent transport of mass across the main thermocline is greater than that both above and below the main thermocline. We suggest, then, that the importance of vertical mixing in maintaining the weakly stratified 15°–18°C water above the main thermocline may be small compared to other processes.

An estimate of the time scale representing the decay of energy via turbulent dissipation in the internal wave field is 25–40 days. This estimate seems consistent with that required for temporal smoothing of internal wave energy levels. Whether this time scale is large enough for spatial smoothing of the IW field depends on a reliable estimate of the horizontal spreading rate of the energy in the field.

Below 1000 m, dissipation rates averaged over 1.3–2 m vertically range from the noise level of the instrumentation to 1.2×10^{-8} m^2 s^{-3} and deep patches as thick as 30 m were observed. The most intense of these had a patch-averaged ϵ of 3×10^{-9} m^2 s^{-3} and was located at 2030 m. The percentage of ϵ estimates greater than 10^{-9} m^2 s^{-3} was 22% over the depth range 400–1000 m, 14% between 1000 and 2000 m and 5% below 2000 m. These values dominate the mean.

Acknowledgments. The captain and crew of the R/V *Thomas G. Thompson* were most helpful in deploying the instrument. Ron Ninnis provided technical help at sea. We have benefited from discussions with Paul Leblond, Ann Gargett and Murray Levine. The constructive comments of Co-Editor Briscoe and two reviewers were gratefully received. As a graduate student at the University of British Columbia, J. N. Moum was supported by a Canadian Natural Sciences and Engineering Research Council Postgraduate Scholarship. This work was sponsored by the Office of Naval Research of the United States.

REFERENCES

Caldwell, D. R., T. M. Dillon and J. N. Moum, 1985: The rapid-sampling vertical profiler: An evaluation. *J. Atmos. Oceanic Technol.*, **2,** 615–625.

Gargett, A. E., 1984: Vertical eddy diffusivity in the ocean interior. *J. Mar. Res.* **42,** 359–393.

——, and T. R. Osborn, 1981: Small-scale shear measurements during the fine and microstructure experiment (FAME). *J. Geophys. Res.*, **86,** 1929–1944.

——, and R. W. Schmitt, 1982: Observations of salt fingers in the central waters of the eastern North Pacific. *J. Geophys. Res.*, **87,** 8017–8029.

——, and G. Holloway, 1984: Dissipation and diffusion by internal wave breaking. *J. Mar. Res.*, **42,** 15–27.

——, T. R. Osborn and P. W. Nasmyth, 1984: Local isotropy and the decay of turbulence in a stratified fluid. *J. Fluid Mech.*, **144,** 231–280.

Garrett, C. J. R., 1984: Parameterizing the effects of internal waves: Simple ideas and things we need to know. *Proc. Hawaiian Winter Workshop,* University of Hawaii, 171–181.

Gill, A. E., 1982: *Atmosphere–Ocean Dynamics.* Academic Press, 662 pp.

Gregg, M. C., 1977: Variations in the intensity of small scale mixing in the main thermocline. *J. Phys. Oceanogr.*, **7,** 436–454.

Larson, N. G., and M. C. Gregg, 1983: Turbulent dissipation and shear in thermohaline intrusions. *Nature,* **306**(5638), 26–38.

Lueck, R. G., W. R. Crawford and T. R. Osborn, 1983: Turbulent dissipation over the continental shelf off Vancouver Island. *J. Phys. Oceanogr.*, **11,** 970–986.

McComas, C. H., and P. Müller, 1981: The dynamic balance of internal waves. *J. Phys. Oceanogr.*, **17,** 1524–1548.

Moum, J. N., 1984: Velocity microstructure measurements in the western and central equatorial Pacific. Ph.D. dissertation, University of British Columbia, 270 pp.

——, and R. G. Lueck, 1985: Causes and implications of noise in oceanic dissipation measurements. *Deep–Sea Res.*, **32,** 379–390.

——, T. R. Osborn and W. R. Crawford, 1986: Pacific equatorial turbulence: Revisited. *J. Phys. Oceanogr.*, **16.**

Munk, W. H., 1966: Abyssal recipes. *Deep–Sea Res.*, **13,** 707–730.

——, 1981: Internal waves and small-scale processes. *Evolution of Physical Oceanography,* B. A. Warren and C. Wunsch, Eds., MIT Press, 264–291.

Niiler, P. P., W. J. Schmitz and D. Lee, 1985: On the geostrophic volume transport in high eddy energy areas off the Kuroshio Extension and Gulf Stream. *J. Phys. Oceanogr.*, **15,** 825–843.

Ninnis, R. M., 1984: The effects of spatial averaging on airfoil probe measurements of oceanic velocity microstructure. Ph.D. dissertation, University of British Columbia, 109 pp.

Oakey, N. S., 1982: Determination of the rate of dissipation of turbulent energy from simultaneous temperature and velocity shear microstructure measurements. *J. Phys. Oceanogr.*, **12,** 256–271.

Osborn, T. R., 1980: Estimates of the local rate of vertical diffusion from dissipation measurements. *J. Phys. Oceanogr.*, **10,** 83–89.

——, and W. R. Crawford, 1980: An airfoil probe for measuring turbulent velocity fluctuations in water. *Air-Sea Interaction,* F. Dobson, L. Hasse and R. Davis, Eds., Plenum, 369–386.

Schmitt, R. W., Jr., and D. L. Evans, 1979: An estimate of the rate of vertical mixing due to salt fingers based on observations in the North Atlantic Central Water. *J. Geophys. Res.*, **83,** 2913–2919.

Schmitz, W. J., Jr., 1984: Observations of the vertical structure of the eddy field in the Kuroshio Extension. *J. Geophys. Res.*, **89,** 6355–6364.

——, P. P. Niiler, R. L. Bernstein and W. R. Holland, 1982: Recent long-term instrument observations in the western North Pacific. *J. Geophys. Res.*, **87,** 9425–9440.

Talley, L. D., and M. E. Raymer, 1982: Eighteen Degree Water variability. *J. Mar. Res.*, **40**(Suppl.), 757–775.